Fluid Motion Between Rotating Concentric Cylinders Using COMSOL Multiphysics™

Kabita Barman[1], Sravanthi Mothupally[1], Archana Sonejee[1], and Patrick L. Mills[*1]
[1]Department of Chemical and Natural Gas Engineering, Texas A&M University-Kingsville
*Corresponding author: Texas A&M University-Kingsville, Department of Chemical & Natural Gas Engineering, EC 303D, MSC 193, 700 University Blvd, Kingsville TX 78363-8202, USA. Email: Patrick.Mills@tamuk.edu

Abstract: A fluid dynamics analysis of the velocity and pressure fields that occur in the annular gap between two concentric cylinders with a stationary outer cylinder and a rotating inner cylinder is presented. Both the transient and steady-state velocity and pressure profiles of an isothermal, Newtonian fluid are considered. The effect of varying the angular velocity of the inner cylinder, fluid viscosity and radius of the inner cylinder on the fluid velocity and pressure profiles are examined. The results show that the fluid velocity profiles approach a fully-developed state only after travelling a distance that is much greater than the annular gap between the cylinders. It is also shown that the pressure exerted on the inner cylinder increases monotonically with rotational speed. Results that illustrate the potential utility of using COMSOL Multiphysics™ to study the fluid flow stability and parametric behaviour are also illustrated.

Keywords: Concentric cylinders, COMSOL Multiphysics™, velocity and pressure profiles, Newtonian fluid, rotational viscometer.

1. Introduction

Fluid-flow patterns in laboratory-scale, pilot-plant scale, and commercial-scale equipment where a fluid is contained between concentric rotating cylinders in the absence of bulk axial flow has received notable attention in fluid mechanics, applied mathematics and chemical engineering. This fluid-solid hydrodynamic contacting pattern, which is often referred to as an *annular flow*, occurs in many practical technology-driven applications, such as in the production of oil and gas, centrifugally-driven separation processes, electrochemical cells, fluid viscometers, tribology, hydraulic equipment, and chemical reactors. Understanding the flow behavior in a vertically-oriented annular gap whose outer wall is stationary while the inner wall rotates is an important problem within the broader scope of fluid flows within annular regions. COMSOL Multiphysics™ provides a modeling platform for investigating various non-ideal effects that can occur in this particular configuration under both transient and steady-state flow conditions. Knowledge of non-ideal effects is important for the design of equipment and interpretation of any derived parameters, such as fluid viscosity, pressure drop, and fluid flow rates.

The primary objective of this study is illustrate the use of COMSOL Multiphysics™ to determine the fluid velocity and pressure profiles between two concentric cylinders in which the inner cylinder is rotating and the outer cylinder is stationary for the case where non-ideal end effects are included. An analytical solution to the simplified 1-D form of the equations of motion for both the transient and steady-state fluid velocity and pressure profiles have been developed, which applies to the case where end effects are neglected (Bird and Curtiss, 1959a, 1959b). The analytical solution for the developing fluid velocity in 1-D is complex and is expressed as an infinite series of Bessel functions. A detailed accounting of end effects, which is required to assess the error incurred for simpler 1-D models, requires a 3-D numerical solution to the Navier-Stokes equations where the assumption of vanishing velocity components in the angular and axial directions is relaxed. Parameters that are varied include the radii of the inner and outer cylinders, rotational speed of the inner cylinder, and kinematic viscosity of the fluid. Conditions that lead to the onset fluid-flow instability are also examined.

2. Description of Physical System

An example of a typical physical system that involves concentric cylinders where one or both

may be rotating occurs in fluid viscometry. Analysis of this particular system has a rich history from the perspectivr of both theory and experiments, which has been partly captured in a series of chapters that appear in an edited monograph (Andereck and Hayot, 1991). A simplified schematic of a Couette viscometer is shown in Figure 1 (Bird *et al.*, 2007). The fluid whose viscosity is to be determined is placed in the cylindrical cup, which is then rotated at a constant angular velocity Ω_o. The cup contains an assembly in the interior that consists of a bob with a set of stationary baffles on the lower and upper region of the cup. The bob is suspended and is connected to a thin vertical torsion wire at the top. The wire is calibrated beforehand and has a known torsion constant k_t. The wire allows the bob to undergo variation in angular rotation θ_o, which is created by the fluid force acting on the outer surface of the bob as a result of momentum transport. The fluid rotation causes the suspended bob to turn until the torque T_{zf} produced by the fluid force acting on the bob is equal to the counter-acting torque defined as product of the torsion constant k_t and the angular displacement θ_o of the bob, *i.e.*, $T_{zw} = k_t\ \theta_o$. Analysis of the fluid motion in the annular region can be performed on

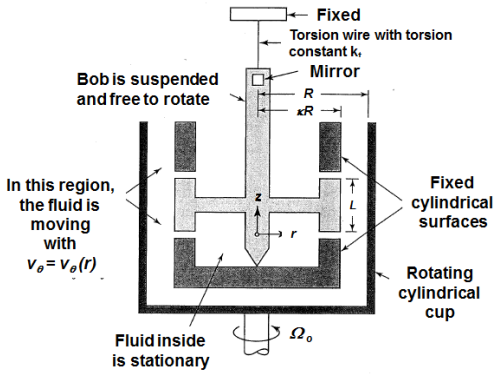

Figure 1. Schematic of a Couette viscometer in which the outer cylinder is rotating and the inner cylinder is stationary. (Adapted from Bird *et al.*, 2007).

various levels of complexity, depending upon the choice of viscometer system design and geometry, fluid properties, and operating conditions (Andereck and Hayot, 1991). In practical applications of Couette viscometry for determination of fluid viscosity, complicating aspects such as fluid instabilities and bifurcation phenomena are to be avoided, although they have rich mathematical properties. Of particular interest here is development of insight into the fluid motion for the case where end effects are included as an entry point for exploring the capabilities of COMSOL Multiphysics™ for system modelling.

3. Governing Equations

3.1 Overview

This section describes the development of the 1-D model for the fluid velocity distribution for the case where the outer cylinder is stationary and the inner cylinder is rotating. The velocity distribution is needed to derive an expression for the torque, which is the working relationship used to extract fluid viscosity data from experimental measurements of the torque versus rotational speed. The analytical expression for the velocity distribution also provides the basis for an initial estimate for the 3-D velocity field.

3.1 Equation of continuity

The equation of continuity for cylindrical coordinates (r,θ,z) is given by (Bird *et al.*, 2007)

$$\frac{\partial \rho}{\partial t} + \frac{1}{r}\frac{\partial (\rho r v_r)}{\partial r} + \frac{1}{r}\frac{\partial (\rho v_\theta)}{\partial \theta} + \frac{\partial (\rho v_z)}{\partial z} = 0$$

If end effects are neglected, the velocity distribution in the angular direction can be assumed to mainly depend upon the radial coordinate. Hence, the contribution of the radial v_r and axial v_z components of the velocity vector $\mathbf{v} = [v_r\ \ v_\theta\ \ v_z]$ can be assumed to be negligible so that $v_r = v_z = 0$ and $v_\theta = v_\theta\ (t,\ r)$ where the dependence on time t is included for the transient solution. In addition, the fluid density is invariant since the fluid is maintained at a constant temperature. With these assumptions, the equation of continuity reduces to

$$\frac{\partial (v_\theta)}{\partial \theta} = 0$$

3.2 Equation of motion

The equations of motion in cylindrical coordinates (r,θ,z) for a Newtonian fluid with constant density and viscosity are given by Bird *et al.* (2007). The components of these equations

are summarized below where all components of the velocity vector **v** = [v_r v_θ v_z] are included. The reduced forms are then given for the 1-D case where $v_r = v_z = 0$ and $v_\theta = v_\theta(r,t)$.

r - component:

$$\rho\left(\frac{\partial v_r}{\partial t}+v_r\left(\frac{\partial v_r}{\partial r}\right)+\frac{v_\theta}{r}\left(\frac{\partial v_r}{\partial \theta}\right)+ v_z\left(\frac{\partial v_r}{\partial z}\right)-\frac{v_\theta^2}{r}\right)=-\left(\frac{\partial p(r,z)}{\partial r}\right)+\rho g_r+ \mu\left(\frac{\partial}{\partial r}\left(\frac{1}{r}\frac{\partial(rv_r)}{\partial r}\right)+\frac{1}{r^2}\frac{\partial^2 v_r}{\partial \theta^2}+\frac{\partial^2 v_r}{\partial z^2}- \frac{2}{r^2}\left(\frac{\partial v_\theta}{\partial \theta}\right)\right)$$

θ – component:

$$\rho\left(\frac{\partial v_\theta}{\partial t}+v_r\left(\frac{\partial v_\theta}{\partial r}\right)+\frac{v_\theta}{r}\left(\frac{\partial v_\theta}{\partial \theta}\right)+ v_z\left(\frac{\partial v_\theta}{\partial z}\right)+\frac{v_r v_\theta}{r}\right)=-\frac{1}{r}\left(\frac{\partial p(r,z)}{\partial \theta}\right)+ \rho g_\theta+\mu\left(\frac{\partial}{\partial r}\left(\frac{1}{r}\frac{\partial(rv_\theta)}{\partial r}\right)+\frac{1}{r^2}\frac{\partial^2 v_\theta}{\partial \theta^2}+ \frac{\partial^2 v_\theta}{\partial z^2}+\frac{2}{r^2}\left(\frac{\partial v_r}{\partial \theta}\right)\right)$$

z-component:

$$\rho\left(\frac{\partial v_z}{\partial t}+v_r\left(\frac{\partial v_z}{\partial r}\right)+\frac{v_\theta}{r}\left(\frac{\partial v_z}{\partial \theta}\right)+ v_z\left(\frac{\partial v_z}{\partial z}\right)\right)=-\left(\frac{\partial p(r,z)}{\partial z}\right)+\rho g_z+ \mu\left(\frac{1}{r}\frac{\partial}{\partial r}\left(r\frac{\partial v_z}{\partial r}\right)+\frac{1}{r^2}\frac{\partial^2 v_z}{\partial \theta^2}+\frac{\partial^2 v_z}{\partial z^2}\right)$$

In the above equations, the z-coordinate is assumed to have an origin as shown in Figure 1 with the positive direction being upward.

Applying the assumptions given above for the velocity components, along with the reduced form of the equation of continuity, generates the following simplified component forms for the equations of motion.

r-component:

$$-\frac{\rho v_\theta(r,\theta)^2}{r}=-\left(\frac{\partial p(r,z)}{\partial r}\right)$$

θ – component:

$$\mu\left(\frac{\partial}{\partial r}\left(\frac{\frac{\partial}{\partial r}\left(rv_\theta(\theta,r)\right)}{r}\right)\right)=0$$

z-component:

$$\frac{\partial p(r,z)}{\partial z}=-\rho g_z \quad \text{(z points upwards)}$$

3.3 Boundary conditions and solutions

The boundary conditions (BCs) are that the fluid does not slip at the surface of the two cylindrical surfaces. When the outer cylinder is rotating and the inner cylinder is fixed, then the BCs are:

B.C. 1 at r = κR, $v_\theta = 0$
B.C. 2 at r = R, $v_\theta = \Omega_o R$

Solving the θ component of the equation of motion given above using these BCs yields

$$v_\theta(r)=\Omega_0 R\left(\frac{\left(\frac{r}{\kappa R}-\frac{\kappa R}{r}\right)}{\left(\frac{1}{\kappa}-\kappa\right)}\right)$$

Another operating mode occurs when the outer cylinder is fixed and the inner cylinder is rotating at Ω_i. The BCs for this case then become

B.C. 1 at r = κR, $v_\theta = \Omega_i R$
B.C. 2 at r = R, $v_\theta = 0$

Following a similar process for solving the θ component of the equation of motion using these BCs results in the following expression for $v_\theta(r)$

$$v_\theta(r)=\Omega_i \kappa R\left(\frac{\left(\frac{R}{r}-\frac{r}{R}\right)}{\left(\frac{1}{\kappa}-\kappa\right)}\right)$$

3.4 Determination of the torque

The momentum flux for the case where the outer cylinder is rotating and the inner cylinder is fixed is defined as

$$\tau_{r\theta}=-\mu\frac{d}{dr}\left(\frac{v_\theta}{r}\right)=-2\mu\Omega_0\left(\frac{R}{r}\right)^2\left(\frac{\kappa^2}{1-\kappa^2}\right)$$

The torque imparted by the fluid acting on the inner cylinder is defined as the product of the total force acting on the surface of the inner cylinder and the lever arm. The total force is determined by evaluating the inward pointing momentum flux ($-\tau_{r\theta}$) at the surface of the cylinder, and then multiplying this result by the total external surface area of the cylinder with the lever arm. The final result is:

$$T_z = (-\tau_{r\theta})\big|_{r=\kappa r}(2\pi\kappa RL)(\kappa R) = 4\pi\mu\,\Omega_0 R^2\,L\left(\frac{\kappa^2}{1-\kappa^2}\right)$$

This torque-based upon this formula would be the value measured if end effects were negligible since it is based on the assumption that $v_\theta = v_\theta(r)$. Analysis of the 3-D flow field is required to assess the deviation from the assumed ideal behavior.

4. Use of COMSOL Multiphysics

CFD is extensively used to predict and analyze the behavior of fluid flows in complex geometries. COMSOL Multiphysics™ is particularly useful to analyze systems involving various multiphysics, such as combined fluid flow, energy transport, and species transport. In connection with the current investigation, Buehler and Louw (2008) used COMSOL to investigate the behavior of spherical gap flows using two concentric spheres. The results showed the non-uniqueness of the supercritical solutions and interesting aspects of the connected bifurcations.

5. Numerical Method

The 3-D geometry of concentric rotating cylinder system where the inner cylinder is rotating and outer cylinder is stationary was developed by using the COMSOL Computational Fluid Dynamics (CFD) module for determination of the velocity and pressure profiles. A typical meshed geometry is shown in Figure 2.

The model parameters are tabulated in Table1. For simplicity, the fluid flowing in the annular region is assumed to be water. The physical parameters for water are given in Table 2.

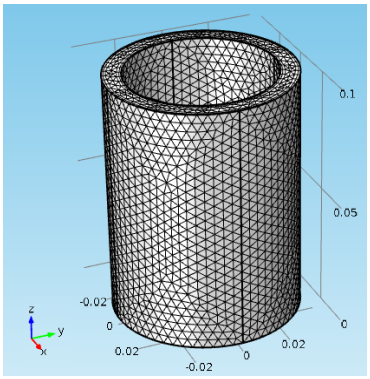

Figure 2. Meshed Geometry

Table 1: Model Parameters

Name	Symbol	Value
Outer Cylinder Radius	R_1	1.5 [in]
Inner Cylinder Radius	R_2	1.2 [in]
Height of the Cylinder	H	10 [cm]
Rational Speed of Inner Cylinder	Ω	1000 [1/min]

Table 2: Transport Parameters for Water

Name	Symbol	Value
Viscosity	μ	0.1 [Pa.s]
Density	ρ	0.918 [kg/m^3]

6. Results and Discussion

Simulations were performed to determine the effect of the inner cylinder angular velocity and the radius of the inner cylinder (and hence the width of the annular gap width) on the fluid velocity, torque and pressure profiles under laminar flow conditions. Selected results are summarized below.

6.1 Pressure profiles

The pressure profiles for the coaxial cylindrical rotational viscometer where the inner cylinder rotates are compared in Figure 3 and 4 for rotational speeds of 55 and 555 RPM, respectively. The initial pressure for the system was taken as 1 atm. The results in Figure 3,

which correspond to 55 RPM, show that the pressure difference is on the order of 1.0 x 10^{-3}. When the rotational speed is increased by an order-of-magnitude to 555 RPM, a pressure difference of ca. 40 x 10^{-3}, is produced, which is almost a factor of 50 greater than that produced at 55 RPM.

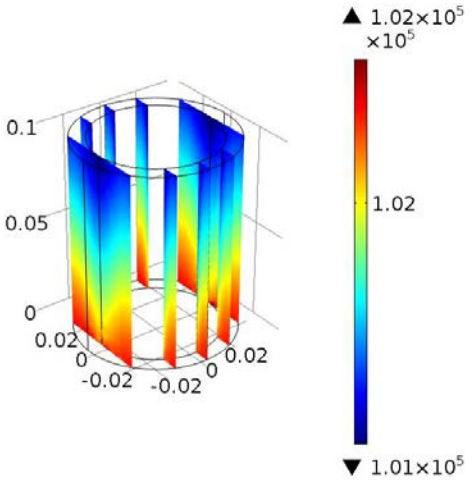

Figure 3. Pressure profile of the fluid at viscometer rotational speed of 55rpm and time 5 secs

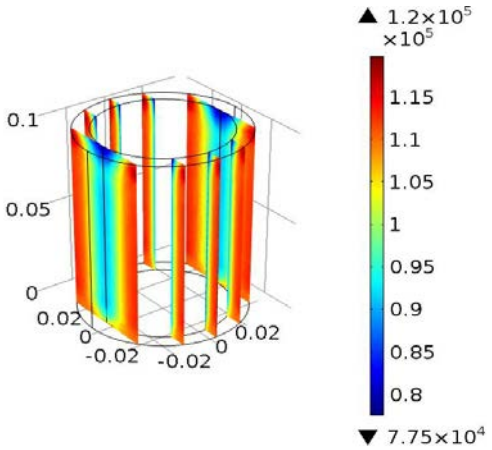

Figure 4. Pressure profiles of the fluid at a viscometer rotational speed of 555 rpm and time 5 secs.

6.2 Velocity profiles

The velocity profiles for the fluid at different heights in the viscometer in the annular region are shown in Figures 6. As expected, the velocity profile at the bottom of the cylinder is not fully developed. However, it appears to approach a fully-developed profile only as the top rim of the viscometer is reached since the profiles at intermediates heights are still evolving. Also, the highest velocity is clearly at the surface of the inner rotating cylinder with zero velocity at the stationary outer cylinder as expected.

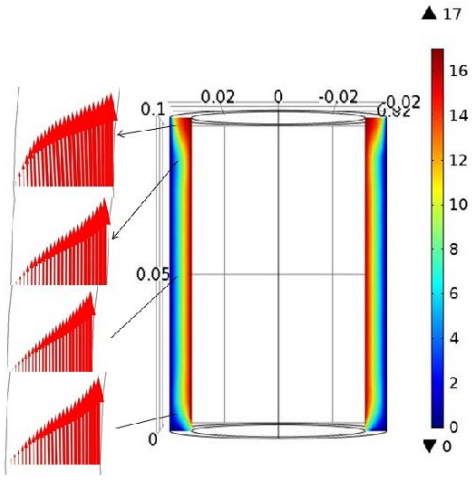

Figure 6. Velocity profile of the fluid at different heights in annular gap of viscometer at 555 rpm and 5 secs

6.3 Effect of varying the inner cylinder radius.

Figure 7 shows the effect of increasing the width of the annular gap by decreasing the radius of the inner rotating cylinder while keeping the outer cylinder radius constant. The fluid velocity decreases with an increase in the annular gap so the flow is deeper in the laminar flow regime.

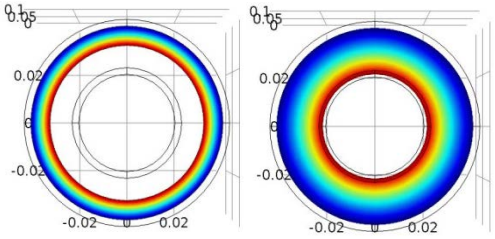

a. **b.**

Figure 7. Velocity profiles of fluid when the inner radius is varied. Fig. 7a**:** R_i = 0.035; Fig.7b**:** R_i = 0.020.

6.4 Fluid velocity profiles

The 3-D graphical perspectives are very helpful in understanding the effect of various fluid properties, system geometry, and operational parameters on the system behavior.

However, 1-D plots of the velocity profiles at selected heights of the cylinders also provide useful insight. Various parameters were varied in order to study this behavior. Figure 8 shows the height at which the velocity profiles were evaluated.

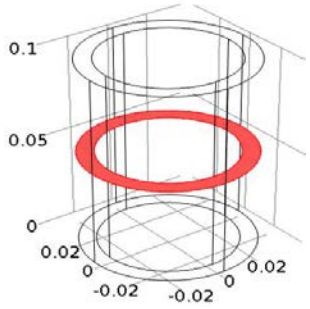

Figure 8. Height at which the velocity profiles were evaluated (0.05 m).

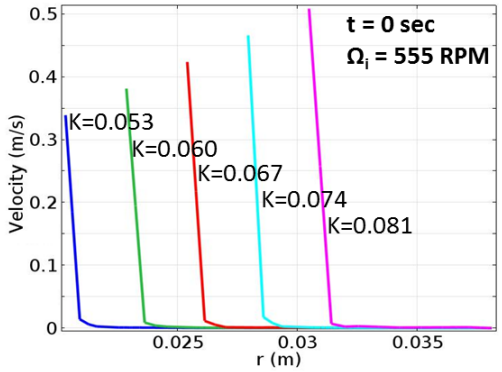

Figure 9. Effect of inner cylinder on fluid velocity profiles at 555 rpm and t = 0 secs.

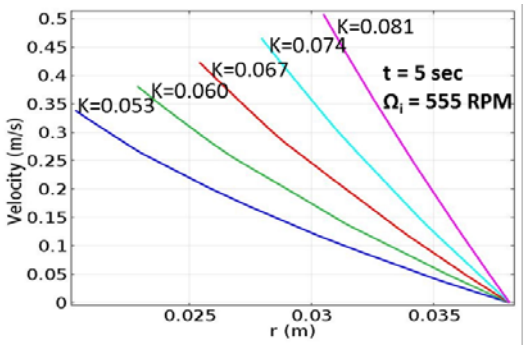

Figure 10. Effect of inner cylinder on fluid velocity profiles at 555 rpm and t = 5secs

Figures 9 and 10 show the velocity (in m/s) at various annular gaps (in m) corresponding to t = 0 and at t = 5 sec, respectively. The results at t = 0 correspond to the initial startup of the cylinder. It can be clearly seen that the initial velocity profiles are steeper that those at 5 sec.

Figure 11 shows how the velocity profiles develop during startup of the inner cylinder. When the cylinder speed varies from a resting state at t = 0 to an instantaneous set point of 55 RPM, the velocity profile varies rapidly. Consequently, the velocity profiles at t = 0.5 s and t = 5 sec overlap, which suggests that the velocity profile has approached a steady-state distribution.

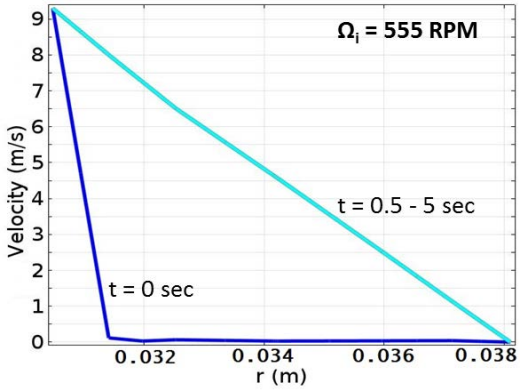

Figure 11. Developing velocity profiles during inner cylinder start up

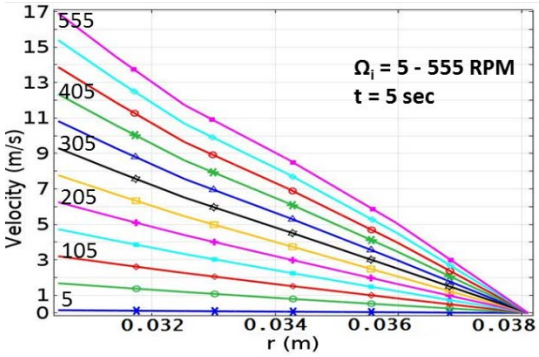

Figure 12. Velocity profiles in the annulus at various rotational speeds and t = 5secs

6.5 Determination of the torque

As explained earlier, the torque imparted by the fluid acting on the inner cylinder is defined as the product of the total force acting on the

surface of the inner cylinder and the lever arm. The equation given above section 3.4 applies to the case where the velocity $v_\theta = v_\theta(r)$ so that end effects are neglected. The resulting equation for the torque shows that collection of torque T_z versus rotational speed Ω_0 data would result in a linear relationship with a slope equivalent to the fluid viscosity for the given temperature. It is evident that a viscometer instrument whose end effects are negligible is desirable since the data interpretation is simplified.

In the current analysis, it is shown that determination of end effects requires solution of the 3-D form of the Navier-Stokes equations. Consequently, the fluid shear stress at the cylinder wall is no longer invariant along the cylinder surface. Hence, determination of the force requires integration of the shear stress at the cylinder surface over the height of the cylinder. These results are discussed elsewhere (Barman *et al*., 2015).

7. CONCLUSIONS

COMSOL Multiphysics™ was used to study the fluid behavior in an annular region between where two concentric cylinders where the inner cylinder was rotating while the outer cylinder was stationary. Solution of the 3-D Navier-Stokes equations in the laminar flow region shows the presence of non-ideal fluid velocity profiles on each end. The flow approaches a fully-developed laminar profile only after traveling a distance that is several times the annular gap width. The analytical solution for the case where the fluid velocity profile depends only on the azimuthal component of the velocity vector in the radial direction agrees with the 3-D solution in the fully-developed zone. It is also shown that the pressure gradient increases with increasing rotational speed. The COMSOL model provides a starting basis for applications involving non-newtonian fluids, such as those used in natural gas drilling muds, polymers and other complex fluids.

8. Nomenclature

R_1 radius of the outer cylinder, m
R_2 radius of the inner cylinder, m
H height of the cylinder, m
p fluid pressure, kg/m.sec^2
v velocity, m/sec
r radial coordinate in cylindrical coordinate, m
z axial coordinate in cylindrical coordinate, m

Greek Letters

Θ arctan (y/x) angle in cylindrical coordinates, radians
ρ density, kg/m^3
μ viscosity, Pa-s
ω rotational speed of the inner cylinder, min^{-1}
v_r, v_θ, v_z velocities in cylindrical coordinates
g_r, g_θ, g_z acceleration due to gravity in cylindrical coordinates, m/s^2

8. References

1. A. M. Sharf., H. A. Jawan. and Fthi A. Almabsout, The influence of the tangential velocity of inner rotating wall on axial velocity profile of flow through vertical annular pipe with rotating inner surface, *EPJ Web of Conferences* 67,02105 (2014)
2. R. B. Bird and C. F. Curtiss, Tangential Newtonian flow in annuli-I, *Chem. Eng. Sci.* 11, pp.108-113 (1959)
3. E. V. Podryabinkin and V. Ya. Rudyak, Moment and forces exerted on the inner cylinder in eccentric annular flow, *Journal of Engineering Thermophysics*, 20, 3, pp.320-328 (2011).
4. J. M. Nouri and J. H. Whitelaw, Flow of Newtonian and non-Newtonian fluids in an eccentric annulus with rotation of the inner cylinder, Int. J. Heat and Fluid Flow, 18, 2, April 1997
5. R. B. Bird *et al.*, Transport Phenomena, 2nd Edn., Wiley, New York (2007)
6. K. Barman, S. Mothupally, A. Sonejee, and P. L. Mills, "Fluid Motion Between Rotating Concentric Cylinders Using COMSOL Multiphysics," Oral presentation given at the COMSOL 2015 Conference, Boston, session on Computational Fluid Dynamics, October 8, 2015.